RGNZ/MGPB

# Assessment of ultra-low frequency (ULF) geomagnetic phenomena associated with earthquakes in the western part of Java Island, Indonesia during 2020

Rudarsko-geološko-naftni zbornik
(The Mining-Geology-Petroleum Engineering Bulletin)
UDC: 550.3
DOI: 10.17794/rgn.2024.1.6

Original scientific paper

**Cinantya Nirmala Dewi[1]; Febty Febriani[1]; Titi Anggono[1]; Syuhada[1]; Mohamad Ramdhan[1]; Mohammad Hasib[1]; Aditya Dwi Prasetio[1]; Hendra Suwarta Suprihatin[2]; Suaidi Ahadi[2]; Mohammad Nafian[3]; Suwondo[3]; Faiz Muttaqy[1]; Muhamad Syirojudin[2]; Hasanudin[2]; Indah Marsyam[2]**

*[1] Research Center for Geological Disaster, National Research and Innovation Agency (BRIN), Jl.Sangkuriang Dago, Bandung 40135, Indonesia, https://orcid.org/0000-0003-1327-2286 (C.N.D.); https://orcid.org/0000-0002-0232-1559 (F.F.); https://orcid.org/0000-0003-1210-6972 (T.A.); https://orcid.org/0000-0001-9505-2361 (S); https://orcid.org/0000-0002-3677-9883 (M.R.); https://orcid.org/0000-0002-3560-4547 (M.H.); https://orcid.org/0000-0002-0844-1711 (A.D.P.); https://orcid.org/0000-0001-5458-5364 (F.Z.)*

*[2] Indonesian Agency for Meteorological, Climatological, and Geophysical (BMKG), Jl.Angkasa I No.2 Kemayoran, Jakarta Pusat 10610, Indonesia, https://orcid.org/0000-0002-9987-3084 (H.S.S.); https://orcid.org/0000-0002-0739-233X (S.A.); https://orcid.org/0000-0002-3170-7223 (M.S.); https://orcid.org/0009-0006-7801-0550 (H); https://orcid.org/0000-0003-0424-884X (I.M.)*

*[3] Physics Department, Syarif Hidayatullah State Islamic University, Jl.Lkr Kampus UIN Ciputat Timur, Tangerang Selatan 15412, Indonesia, https://orcid.org/0009-0009-5076-1768 (M.N.); https://orcid.org/0009-0005-9329-5737 (S)*

## Abstract

Ultra-low frequency (ULF) geomagnetic analysis is a robust method for earthquake (EQ) forecasting. We conducted a simultaneous study of EQ precursors around the western part of Java Island in 2020 using wavelet transform (WT) and detrended fluctuation analysis (DFA) methods. ULF geomagnetic data (March to December 2020, 16:00–21:00 UTC or 23.00–04.00 LT) from Lampung Selatan (LPS) geomagnetic station were used to assess the precursors. We analyzed four EQs with an epicenter distance (R) of around 100 km from LPS station and a magnitude (M) greater than 5 Mw. We analyzed changes in the $S_Z/S_G$ values and $\alpha$ values from the WT and DFA analyses against the threshold ($\mu \pm 2\sigma$) to identify anomalies related to the EQs. The result showed that $S_Z/S_G$ anomalies occurred simultaneously with a decrease in $\alpha$ values several weeks prior to probable source EQ when there was a very low geomagnetic activity (Dst $\leq$ -30 nT). The Mw5.4 (07/07/2020) EQ might be the main source that led to the appearance of the precursor since it had the highest magnitude and $K_{LS}$ values compared to others. The combined WT and DFA results showed anomalies 1.5–13 weeks before the Mw5.4 (07/07/2020) EQ. The results suggest that WT and DFA are suitable methods for detecting EQ precursors but more work is needed to link the precursors to specific EQs.

**Keywords:**
earthquake precursor; ULF emission; wavelet transform analysis; detrended fluctuation analysis

## 1. Introduction

Indonesia has a complex geological structure with several active faults that can become the location of an earthquake (EQ) source, since it is placed at the intersection of the Indo-Australian, Pacific, and Eurasian Plates. Among the active EQ areas in Indonesia is the western part of Java Island, which includes the West Java and Banten provinces. The Indonesian Agency for Meteorological, Climatological, and Geophysical (BMKG) reported 4,253 EQs with a magnitude (M) > 3 have occurred in these two provinces during 2009-2019 (**Sabtaji, 2020**). Based on Statistics Indonesia (BPS) data, almost 54 million people live in the West Java and Banten provinces (**Statistics Indonesia, 2020**). The high frequency of the EQs and the population size make it very important to conduct an immediate EQ hazard assessment in the western part of Java to reduce fatalities and material damage. The short-term EQ forecast is one tool used for EQ risk mitigation, created by investigating the ultra-low frequency (ULF) precursors related to EQs.

The EQ preparation process is correlated with the induced magnetic field, which reflects changes in the electrical structure. However, it has a weak intensity and is usually combined with environmental disturbance and external geomagnetic variation (**Yao et al., 2022**). In the EQ precursor studies, the use of ULF (0.01–0.1 Hz) data could prevent the external geomagnetic variation produced by lightning discharge and ionospheric heating radiation from interfering with EQ precursor analysis (**Yusof et al., 2021**). In addition, natural geomagnetic

---

Corresponding author: Cinantya Nirmala Dewi and Febty Febriani
*cina001@brin.go.id; cinanthiia@gmail.com; febt001@brin.go.id*

emission decreases with increasing frequency, meaning it is preferable to choose a lower frequency to observe seismomagnetic signals (**Hayakawa et al., 2019**). **Hayakawa et al. (1996)** introduced the spectral density ratio (SDR) to analyze the geomagnetic anomaly before an EQ, which was effective in eliminating the global geomagnetic effects. The SDR method divides the vertical geomagnetic field by the horizontal geomagnetic field.

Globally, several previous studies have proven that geomagnetic anomalies at ULF can be used in research related to EQ precursors (e.g. **Hayakawa et al., 2007, 2019, 2022; Han et al., 2014, 2017, 2020; Hattori et al., 2013; Potirakis et al., 2019, 2021; Yusof et al., 2019a, 2019b, 2021; Stanica et al., 2019, 2021; Chen et al., 2020; Warden et al., 2020; Singh et al., 2020; Ozsoz and Pamukcu, 2021; Heavlin et al., 2022; Yao et al., 2022; Marzuki et al., 2022; Feng et al., 2022**). This is due to the low attenuation and deep penetration capability of the ULF geomagnetic signal (**Han et al., 2014; Yusof et al., 2021; Yao et al., 2022**). Assessment of EQ precursors using the geomagnetic method has also been developed in Indonesia for EQs with Mw ≥ 5 (**Febriani et al., 2014, 2020; Ramadhani et al., 2019; Sokacana et al., 2019; Dewi et al., 2020, 2022; Marzuki et al., 2022**). On Java Island, previous research conducted a precursor assessment for the Mw7.5 EQ in Tasikmalaya that occurred on September 2, 2009, based on geomagnetic data from the Pelabuhan Ratu (PLR) station in West Java using wavelet transform (WT) and detrended fluctuation analysis (DFA). The geomagnetic anomalies for the Tasikmalaya EQ were identified a week before the EQ (**Febriani et al., 2014**). In addition, research related to the Mw6.1 Lebak, Banten EQ was conducted using the fast Fourier transform (FFT) method based on geomagnetic ULF data from Serang station, Banten. The anomaly was detected two weeks before the Mw6.1 and is suspected to have been related to the EQ (**Febriani et al., 2020**).

The $E_S$ parameter can be used to increase the probability of identifying ULF geomagnetic anomalies before an EQ. It considers the EQ hypocenter, station distance, and magnitude. The $E_S$ parameter was used to calculate the energy released by EQs (**Hattori et al., 2006**). To increase the probability of ULF geomagnetic appearance, Hattori determined the event day based on an epicenter distance of within 100 km of the station and the value of daily local EQ energy ($E_S$) exceeding $10^8$ (**Hattori et al., 2013**). Statistical tests successfully proved the EQ selection criteria by indicating the presence of ULF geomagnetic anomalies when the value of $E_S$ is $> 10^8$ and the epicenter distance is < 100 km (**Han et al., 2014**).

In this research, we used WT and DFA analyses to analyze the EQ precursors around the western part of Java Island. The correlation between the WT and DFA analyses can assist in determining the most effective method for analyzing EQ precursors. We also aimed to prove the effect of epicenter distance and $E_S$ values on the probability of detecting EQ precursors. The ultimate goal of this research is to demonstrate the validity of EQ characteristics based on EQ precursor analysis in the western part of Java Island and to contribute to global research related to disaster hazard assessment. A good understanding of EQ characteristics will help in planning for optimized EQ disaster hazard reduction efforts, especially in strategic development areas such as the western part of Java Island.

## 2. Data and Methods

ULF geomagnetic data were received from Lampung Selatan (LPS) station, Sumatra (5.789°S, 105.583°E). This magnetometer is operated by BMKG. The EQs selected for observation were filtered by their magnitude and radius from LPS station. We used the following criteria: the selected EQs must have occurred around 100 km from LPS station with an Mw ≥ 5 and $E_S > 10^8$ to increase the probability of detecting their precursor (**Han et al., 2014**). The $E_S$ parameter takes into account the hypocenter distance and the magnitude of selected EQ events and is defined by the calculation given in **Equations 1** and **2** as follows (**Hattori et al., 2006**):

$$E_S = \sum\nolimits_{1\,day} E_S^{'} \tag{1}$$

$$E_S^{'} = \frac{10^{4.8+1.5M}}{r^2} \tag{2}$$

Where:

$E_S$ - daily sum of the local EQ energy (J/km$^2$),

$E_S^{'}$ - local EQ energy (J/km$^2$),

$M$ - EQ magnitude (Mw),

$r$ - hypocenter distance (km).

A previous study also suggested calculating the local seismicity index ($K_{LS}$) to represent the magnitude and distance of an EQ (**Molchanov and Hayakawa, 2008**). Moreover, another previous study stated that an EQ with a high $K_{LS}$ value in a series of EQs is considered the primary source of the precursor (**Yusof et al., 2019b**). The $K_{LS}$ value is defined by **Equation 3** as follows:

$$K_{LS} = \frac{10^{0.75M}}{R+100} \tag{3}$$

Where:

$K_{LS}$ - local seismicity index,

$M$ - EQ magnitude (Mw),

$R$ - epicenter distance (km).

We used data from relocated EQ catalog of BMKG as a reference for selecting the EQs (**Ramdhan et al., 2021**). The teleseismic double-difference method and regional 3-D velocity models were used to obtain more precise hypocenter parameters (longitude, latitude, depth, and time of EQ occurrence) according to the ac-

**Table 1:** EQs with Mw ≥ 5 around the western part of Java Island in 2020

| Date | Time (UTC) | Lat (N) | Long (E) | Mag (Mw) | Depth (km) | R (km) | $K_{LS}$ | $E_S$ (Joule/km$^2$) |
|---|---|---|---|---|---|---|---|---|
| 10/02/2020 | 05:22:54.32 | -6.908 | 105.289 | 5 | 11.06 | 128.847 | 24.573 | 1.19E+08 |
| 03/05/2020 | 07:06:46.33 | -6.316 | 104.676 | 5.3 | 48.648 | 116.791 | 43.547 | 3.51E+08 |
| 07/07/2020 | 04:44:13.45 | -6.686 | 106.176 | 5.4 | 97.362 | 119.696 | 51.071 | 3.34E+08 |
| 14/07/2020 | 00:04:34.77 | -6.914 | 106.172 | 5.3 | 96.975 | 141.380 | 39.111 | 1.91E+08 |
| 25/08/2020 | 11:27:59.32 | -6.680 | 104.616 | 5.3 | 47.878 | 146.424 | 38.310 | 2.37E+08 |

tual tectonic conditions (**Pesicek et al., 2010; Widiyantoro and van der Hilst, 1997**). Our search of the relocated EQ catalog of BMKG returned five EQs that met the criteria during 2020, as listed in **Table 1**.

The magnetometer recorded the raw geomagnetic data in the time domain comprising horizontal (X and Y) and vertical (Z) components. The raw data is sampled with a frequency of 1 Hz. We used geomagnetic data recorded in 2020 at LPS station; data were available for the period March 1, 2020, to December 31, 2020. No data were recorded at the station from January 1, 2020, to February 29, 2020, and on March 4, 2020. We then compared the availability of geomagnetic data from LPS station with the EQ data in **Table 1**. Only four EQs could ultimately be analyzed because the Mw5 10/02/2020 EQ occurred during the period when there was no data from LPS station; it was therefore excluded. The position of LPS station and the four analyzed EQs, namely Mw5.3 (03/05/2020), Mw5.4 (07/07/2020), Mw5.3 (14/07/2020), and Mw5.3 (25/08/2020), are shown in **Figure 1**.

We focused on five hours (16:00–21:00 UTC) of nighttime data for analysis to minimize the artificial noise (**Han et al., 2014; Febriani et al., 2014; Yusof et al., 2019b**). **Figure 2** contains an example of nighttime data, recorded by LPS station on March 16, 2020. Then, we performed WT analysis to obtain a localized variation of the power values of three components of geomagnetic data (X, Y, and Z). Signal information can be retrieved simultaneously in the time and frequency domain. The WT analysis applied the SDR method to identify seismogenic emission or to distinguish the seismogenic event from other noise (**Hayakawa and Hattori, 2004**). We used the Morlet wavelet in WT analysis as the mother wavelet to transform the raw data to the frequency domain data, since it is similar to the Fourier transform (**Morlet et al., 1982**). An error exists on the first and last of WT data because of the finite-length time-series nature of the data; this is known as the edge effect of WT (**Febriani et al., 2014**). To avoid this edge effect, we excluded the first and last 30 minutes from the data. Therefore, we only used data for the period 16:30–20:30 UTC for further analysis.

The spectrograms were plotted based on the calculation results of the spectral density values. We then extracted the signal at frequencies of around 0.01–0.06 Hz (±0.003 Hz) to determine the greatest probability of detecting ULF geomagnetic anomalies. A previous study suggested optimum frequency ranges for the appearance of ULF geomagnetic anomalies before EQs of around 0.02–0.03 Hz and 0.06 Hz (**Yusof et al., 2019a**). The daily mean ($\mu_{day}$) value was computed from the average of the spectral density values for every frequency range. After obtaining the daily mean ($\mu_{day}$) value, we continued to compute the monthly mean ($\mu_{month}$) and monthly standard deviation ($\sigma_{month}$). We performed the normalization process on the spectral density value to reduce the monthly trend effect using the calculation given in **Equation 4**. We then obtained the SDR by computing the values of $S_Z/S_X$, $S_Z/S_Y$, and $S_Z/S_G$.

$$S_{day,i} = \frac{\mu_{day,i} - \mu_{month,i}}{\sigma_{month,i}} \tag{4}$$

Where:

| | |
|---|---|
| $S$ | - normalized spectral density values (nT$^2$/Hz), |
| $i$ | - indicates the X, Y, and Z components, |
| $\mu_{day}$ | - daily mean of spectral density values (nT$^2$/Hz), |
| $\mu_{month}$ | - monthly mean of spectral density values (nT$^2$/Hz), |
| $\sigma_{month}$ | - monthly standard deviation of spectral density values (nT$^2$/Hz). |

We also conducted DFA in this study as a comparison and to ensure the persistence of the detected precursor. DFA is powerful for long-range correlation analysis of time series data (**Guzman-Vargaz et al., 2019**) and was used to determine the behaviour of scaling data against existing data trends. The time series data were first integrated to obtain the y(k) profile, which was then split into non-overlapping and equivalent segments of length n. To establish the local trend $y_n(k)$, we fitted a straight line to each segment. Then the integrated and detrended time series on all segments are calculated for the root mean square fluctuations using **Equation 5**.

$$F(n) = \sqrt{\frac{1}{N}\sum\nolimits_{k=1}^{N}\left[y(k) - y_n(k)\right]^2} \tag{5}$$

The relationship between F(n) and n is expressed in terms of power-law scaling given in **Equation 6**.

$$F(n) \sim n^{\alpha} \tag{6}$$

Where:

| | |
|---|---|
| $F(n)$ | - fluctuation function, |
| $n$ | - length of segment, |

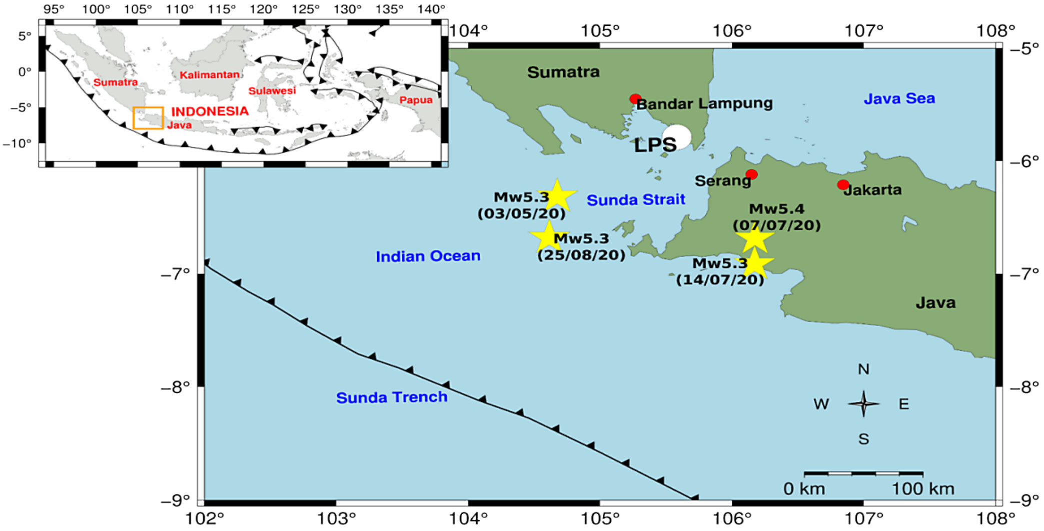

**Figure 1:** The position of LPS station and the analyzed EQs

$N$ - length of the series,
$y(k)$ - integrated time series,
$y_n(k)$ - the y coordinate of the fitting line,
$\alpha$ - scaling exponent.

The slope of F(n) to log n is known as the scaling exponent (α), which expresses the correlation in time series data. The existence of long-range correlation, which indicates a large value (compared to the mean), followed by a large value and vice versa and is indicated by $\alpha > 0.5$. Meanwhile, an anti-persistent long-range correlation, which indicates large values (compared to the mean), followed by small values and vice versa and is indicated by $\alpha < 0.5$ (**Peng et al., 1994; Ida et al., 2006; Telesca et al., 2008**).

We defined $\mu \pm 2\sigma$ as the threshold for the WT and DFA data to define the precursor and reduce ambiguity due to other noise. To ensure that the detected precursors were not associated with global geomagnetic activity, we also plotted the disturbance storm time (Dst) index to be observed simultaneously with the WT and DFA results. The Dst index describes the geomagnetic storm intensity by calculating disturbances of the geomagnetic field in the low latitude and equatorial region (**Saroso et al., 2009; Chen et al., 2020**). A negative Dst index value indicates a weakening of the Earth's magnetic field caused by geomagnetic storms (**Mahmoudian et al., 2022**). Any daily Dst index value $\leq$ -30 nT indicates the existence of a geomagnetic storm (**Gonzales et al., 1994**). Geomagnetic anomalies that occur during geomagnetic storm periods should be ignored since they are caused by geomagnetic environment factors (**Yusof et al., 2019b; Marzuki et al., 2022**). Furthermore, we plotted the $E_S$ and $K_{LS}$ values of the EQs that occurred during 2020 with criteria $Mw \geq 5$, depth $\leq$ 100 km, and $R \leq 150$ km to determine the correlation of magnitude, depth, distance, $E_S$, and $K_{LS}$ on the occurrence of EQ anomalies.

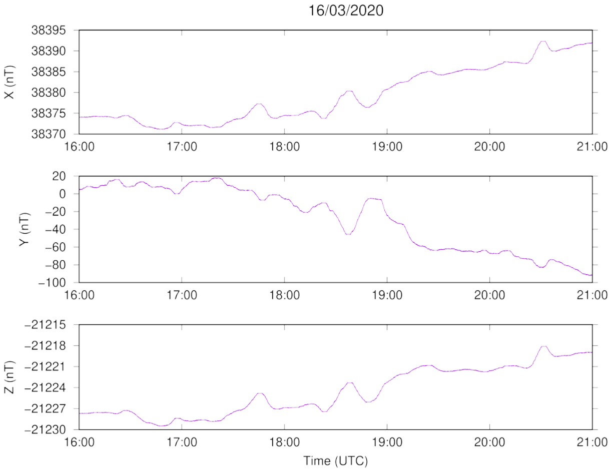

**Figure 2:** An example of nighttime data on March 16, 2020

## 3. Results and Discussion

**Figure 3** presents a WT spectrogram of three components of geomagnetic data on March 16, 2020. To minimize the edge effect, we focused on the area of the WT spectrogram within the red rectangle and ignored the first and the last 30 min of data. The WT spectrogram of the vertical component (Z) is more homogenous than those of the horizontal components (X and Y). This confirms that local geological structures affect the induction fields that appear in the Z component and distinguish it from others (**Hattori et al., 2013; Han et al., 2014, 2020**).

We calculated the spectral density values for three components of geomagnetic data as shown in **Figure 4**. However, the result indicates that no relationship exists between EQ occurrence and the spectral density values. Next, we performed an SDR analysis on the normalized data. We computed the SDR between the Z component and the X, Y, and total horizontal components (G) ($S_Z/S_X$, $S_Z/S_Y$, and $S_Z/S_G$) at 0.01–0.06 Hz in this study, but

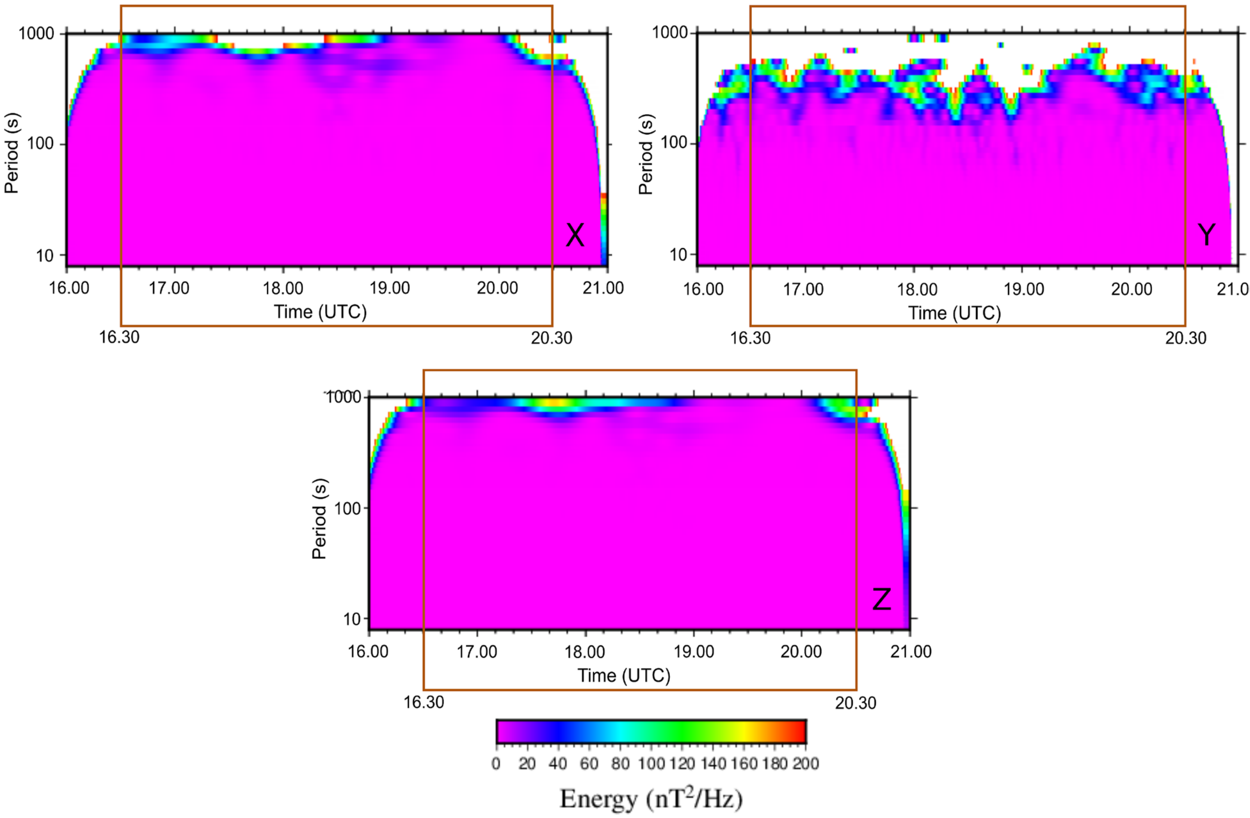

**Figure 3:** Typical WT spectrograms on March 16, 2020

we only focused on the SDR of $S_Z/S_G$ to analyze the correlation between EQ and ULF geomagnetic anomalies. Previous studies have reported that a large EQ can generate an increase in the ULF geomagnetic signal in component Z (**Hattori et al., 2013**). We also detected 0.02 Hz as the optimum frequency to analyze the EQ precursors compared to other frequencies around 0.01 - 0.06 that we observed in this study.

We subsequently performed DFA in this study as a comparison. We applied this to five hours (16:00–21:00 UTC) of nighttime raw data, as in the WT analysis. **Figure 5** presents an example result of fluctuation function based on DFA analysis of three components of geomagnetic data. The behaviour of the fluctuation function forms a straight line where an increase in the value of F(n) is followed by an increase in the value of n. Specifically, due to power-law scaling, F(n) will increase as $F(n) \sim n^{\alpha}$, where α is known as the scaling exponent that will represent the correlation of data (**Peng et al., 1994; Ida et al., 2006; Telesca et al., 2008**).

**Figure 6** shows the results of WT and DFA analyses combined with Dst index, $E_S$, and $K_{LS}$ values. The figure indicates that the SDR of $S_Z/S_G$ significantly exceeds the threshold of $\mu+2\sigma$ from April 27, 2020, to June 26, 2020, which is marked with a blue dashed ellipse. We additionally identified anomalies shortly after Mw5.4 (07/07/2020) and Mw5.3 (14/07/2020), which are marked with a gray dashed circle. We assumed that these were post-EQ anomalies related to the Mw5.4 (07/07/2020) EQ, but they could also be precursors of the Mw5.3 (25/08/2020) EQ. Meanwhile, the anomaly based on the DFA result was observed on April 5, 2020 (marked with a blue dashed square). All of the WT and DFA anomalies were detected during a quiet day of a geomagnetic storm, as detailed in **Table 2**. This indicates that the anomalies were potentially related to the EQ precursors and not produced by global geomagnetic disturbance. We analyzed the depth, epicenter distance, $K_{LS}$, and $E_S$ values from **Table 1** to reveal the main EQ that caused the anomaly. In our case, all analyzed EQs have virtually the same magnitudes, meaning their effect cannot be significantly determined; however, they do have varying depths, epicenter distances, $E_S$, and $K_{LS}$ values. Mw5.4 (07/07/2020) was the deepest EQ but also had the greatest magnitude and the highest $K_{LS}$ compared to the others.

Therefore, we consider that the anomaly emerging from the WT and DFA analysis is the Mw5.4 (07/07/2020) EQ precursor. The anomalies occurred around 1.5–10 weeks and 13 weeks before the Mw5.4 (07/07/2020) EQ based on the WT and DFA results, respectively. **Figure 6** also shows the characteristics of the ULF geomagnetic anomaly before the EQ; this is marked by an increase in the $S_Z/S_G$ value exceeding the threshold of $\mu+2\sigma$ that is accompanied almost simultaneously by a decrease in the α value beneath the threshold of $\mu-2\sigma$. This finding is similar to those of previous studies, which also identified an increase in $S_Z/S_G$ accompanied by a decrease in α value a few weeks before the Mw7.5 EQ in Tasikmalaya on September 2, 2009 (**Febriani et al., 2014**).

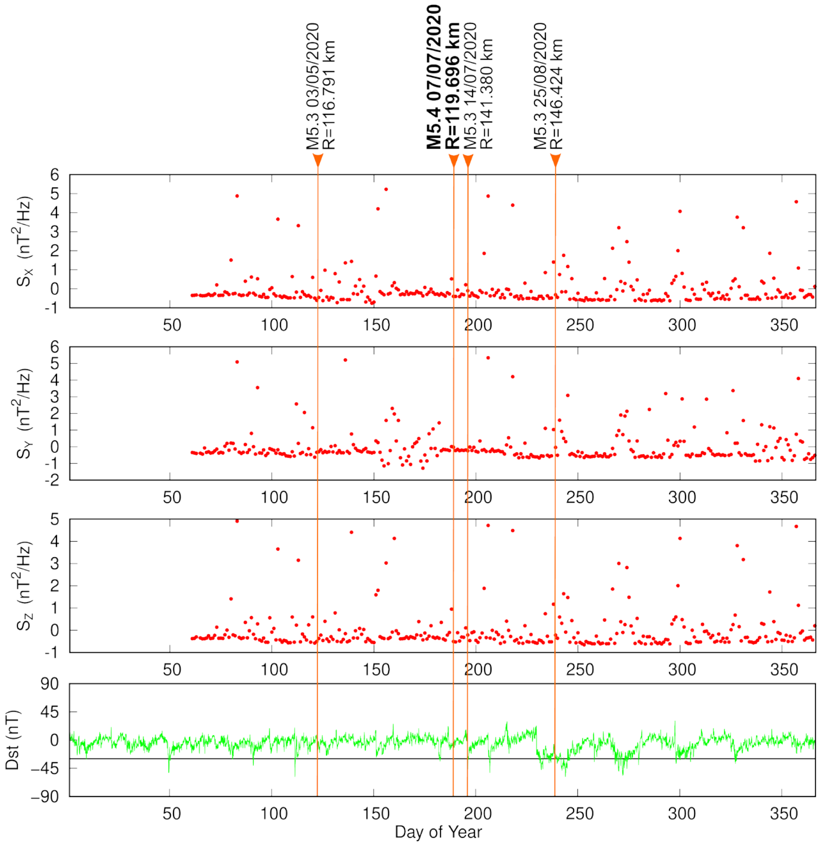

**Figure 4:** Spectral density values of $S_X$, $S_Y$, and $S_G$ at 0.02 Hz

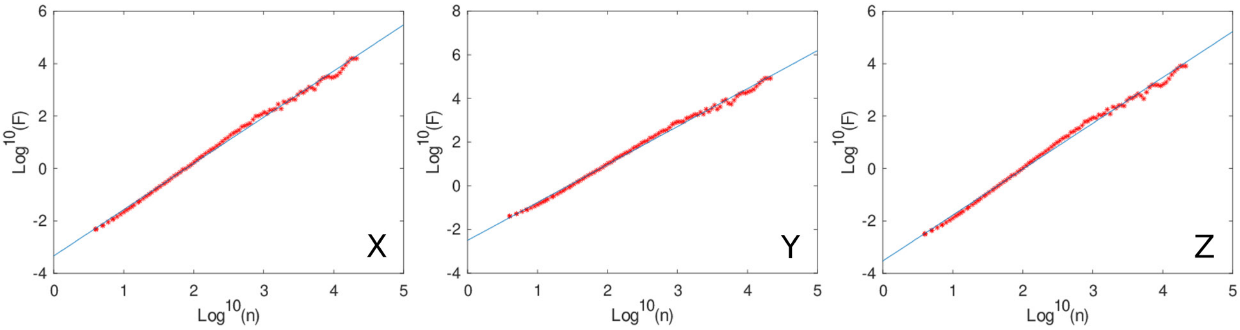

**Figure 5:** Typical log F(n) versus log n plots on March 16, 2020

The Mw5.4 (07/07/2020) EQ, which had the highest $K_{LS}$ value among all of the analyzed EQs, is considered to be the probable principal source for the observed anomalies (**Yusof et al., 2019b**). In addition, the Mw5.3 (03/05/2020) EQ may also have contributed to the appearance of the anomalies on April 27, 2020, from the WT analysis and April 5, 2020, from the DFA analysis because it has a shallower depth, slightly closer epicenter distance, and slightly larger $E_S$ value than the Mw5.4 (07/07/2020) EQ.

The highest $K_{LS}$ value indicates that the EQ is the main cause of the precursors (**Yusof et al., 2019b**). Meanwhile, the Mw5.3 (14/07/2020) and Mw5.3 (25/08/2020) EQs had a smaller likelihood of causing an anomaly due to their greater epicenter distance and lower $E_S$ and $K_{LS}$ values than the Mw5.4 (07/07/2020) EQ. The plots of the $E_S$ and $K_{LS}$ values in **Figure 6** reflect how, throughout 2020, other earthquakes with Mw < 5 that occurred within a 150 km radius of LPS station were analyzed alongside the main earthquakes. The Mw < 5 earthquakes have $E_S < 10^8$ and average $K_{LS}$ values of around 3, meaning they were not strong enough to produce a geomagnetic anomaly. These results confirm that the selection of the parameters of epicenter distance, $K_{LS}$, $E_S$, and depth greatly assist in identifying EQs that may cause ULF geomagnetic anomalies (**Febriani et**

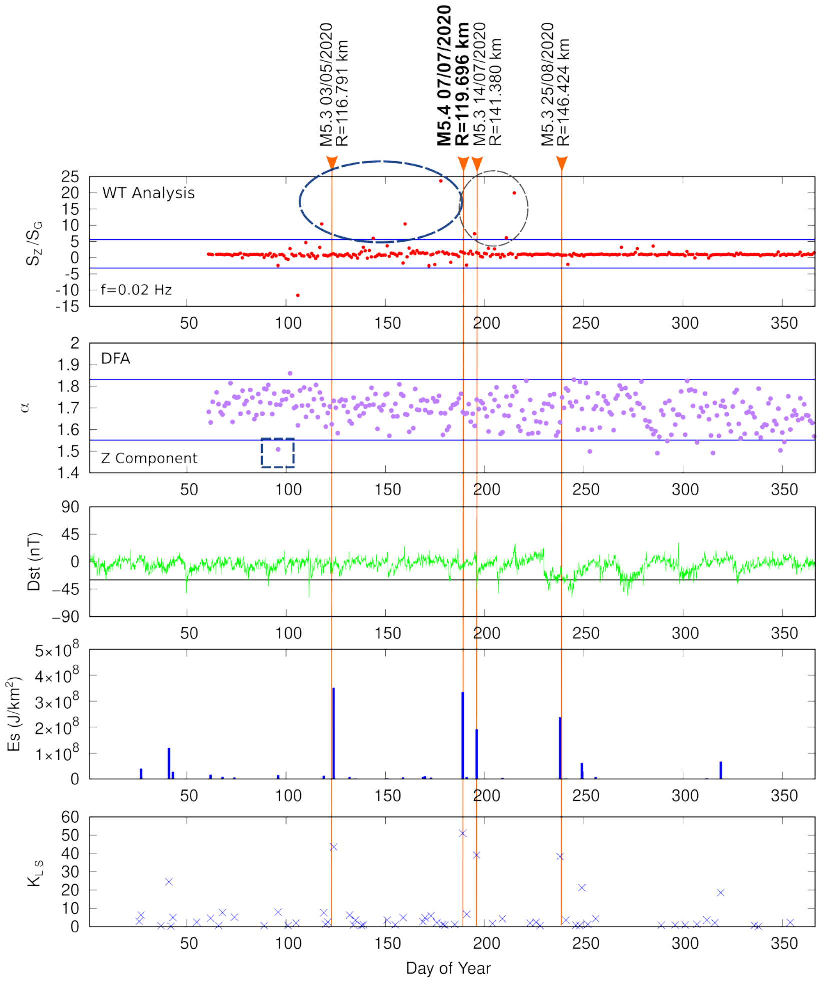

**Figure 6:** Combination of the $S_Z/S_G$ values at 0.02 Hz based on WT analysis, α values based on DFA, Dst index, $E_S$ and $K_{LS}$. The vertical orange lines show the EQ incidents. The horizontal blue lines denote the WT and DFA thresholds (μ±2σ), whereas the black line denotes the Dst index values of -30 nT. The blue dashed ellipse and square indicate geomagnetic anomalies based on WT and DFA analysis, respectively. Meanwhile, the gray dashed circle shows the post-EQ probable anomalies of the Mw5.4 EQ.

**al., 2014; Han et al., 2014, 2017; Yusof et al., 2019a, b; Han et al., 2020; Yao et al., 2022**).

The EQs analyzed in this study stretched from the southwest of Java Island toward the southeast of Sumatra Island, as seen in **Figure 1**. This area is a subduction zone of the Indo-Australian Plate beneath the Sunda Plate in the Sunda-Java Trench (**Hutchings et al., 2021**). EQs in the south of Java and Sumatra Island that led to the Java Trench occurred along the megathrust and several others related to backthrust due to interplate faults at the confluence of the Australian and Sunda plates (**Supendi et al., 2022**).

The high potential for EQs that threaten the western part of Java drives studies related to EQ precursors to play an important role in supporting disaster risk reduction strategies. Long-term precursors in the form of seismic gaps have been identified between the Java coast and the Java Trench, in the south of Java Island, indicating strain accumulation that may cause large EQs accompanied by tsunamis in the future (**Widiyantoro et al., 2020; Supendi et al., 2022**).

Generally, long-term precursors can be observed within several tens to hundreds of years (**Wang, 2020**). Meanwhile, short-term precursors, such as geomagnetic anomalies, may be observed months before an EQ. These geomagnetic anomalies arise due to quasi-static slip on inter-asperity faults (**Wang, 2020**). However, the EQ precursors phenomenon remains a complex and sizeable challenge. While some EQs can show significant precursors, others may not. Therefore, a combination with other studies related to EQ precursors (e.g. the b-value, total electron content (TEC), non-volcanic tremors, and water-level change) is needed to strengthen the analysis in future multidisciplinary research.

## 4. Conclusions

We analyzed geomagnetic data in 2020 from the LPS station to observe the EQ precursors that occurred in the western part of Java Island using the WT and DFA methods. We considered four major EQs in 2020 that met our

**Table 2:** Observed EQ precursors

| Analysis | Threshold | | Date | $S_Z/S_G$ | Daily average of Dst index |
|---|---|---|---|---|---|
| | $\mu+2\sigma$ | $\mu-2\sigma$ | | | |
| WT | 5.572 | -3.192 | 27/04/2020 | 10.432 | -10.042 |
| | | | 23/05/2020 | 5.985 | -7.417 |
| | | | 08/06/2020 | 10.431 | -7.458 |
| | | | 26/06/2020 | 23.693 | 0.875 |
| | | | 13/07/2020 | 7.366 | 5.333 |
| | | | 29/07/2020 | 6.128 | -3 |
| | | | 02/08/2020 | 19.953 | 12.417 |
| DFA | 1.832 | 1.552 | 05/04/2020 | 1.508 | -0.083 |

criteria and data availability. Based on WT analysis, we noticed anomalies in the $S_Z/S_G$ values that surpassed the $\mu+2\sigma$ threshold around 1.5–10 weeks before the EQs at a frequency of 0.02 Hz. Meanwhile, DFA showed that the $\alpha$ values fell below the $\mu-2\sigma$ threshold around 13 weeks before the strongest EQ. The Dst index values revealed that geomagnetic activities were quiet at that time. Our results suggest that the observed anomalies were assumed to be mainly precursors of the Mw5.4 (07/07/2020) EQ because it had the largest magnitude and $K_{LS}$ value. These results show that WT and DFA are suitable methods for detecting EQ precursors. Moreover, they also reveal that the occurrence of anomalies is influenced by magnitude, epicenter distance, $E_S$, and $K_{LS}$ values. However, more work is needed to undoubtedly identify specific anomalies as precursors of a specific EQ.

### *Acknowledgement*

The authors thank the Indonesian Agency for Meteorological, Climatological, and Geophysical (BMKG) for providing the earthquake catalog, and the World Data Center for Geomagnetism of Kyoto University for providing the Dst data. We used Generic Mapping Tools 6 to create the figures in this paper (**Wessel et al., 2019**). This research was funded by the 2021 L'Oreal-UNESCO for Women in Science Program awarded to Febty Febriani and the Disaster Research Program (Grant No. SP DIPA-124.01.1.690501/2022) of the National Research and Innovation Agency (BRIN).

## 5. References

### *Papers:*

Chen, H., Wang, R., Miao, M., Liu, X., Ma, Y., Hattori, K. and Han, P. (2020): A statistical study of the correlation between Geomagnetic Storms and M≥ 7.0 Global Earthquakes during 1957–2020. Entropy, 22, 11, 1270.

Dewi, C.N., Febriani, F., Anggono, T., Soedjatmiko, B., Prasetio, A.D. and Ahadi, S. (2020): The ULF geomagnetic anomalous signal associated with Nias earthquake M5. 3 North Sumatra Indonesia on September 6, 2018. Journal of Physics: Conference Series, 1568, 1, 012027.

Dewi, C.N., Febriani, F., Anggono, T., Syuhada, Hasib, M., Prasetio, A.D., Sulaiman, A., Suprihatin, H.S., Ahadi, S., Syirojudin, M., Hasanudin and Marsyam, I. 2022. The optimum frequency for detecting earthquake precursors based on ultra-low frequency (ULF) geomagnetic data from Sukabumi (SKB) station. AIP Conference Proceedings 2652(1): 030004.

Febriani, F., Anggono, T., Syuhada., Prasetio, A.D., Dewi, C.N., Hak, A.S. and Ahadi, S. (2020): Investigation of the ultra low frequency (ULF) geomagnetic anomalies prior to the Lebak, Banten earthquake (M= 6.1; January 23, 2018). AIP Conference Series, 2256, 1, 090002.

Febriani, F., Han, P., Yoshino, C., Hattori, K., Nudiyanto, B., Effendi, N., Maulana, I., Suhardjono and Gaffar, E. (2014): Ultra low frequency (ULF) electromagnetic anomalies associated with large earthquakes in Java Island, Indonesia by using wavelet transform and detrended fluctuation analysis. Natural Hazards and Earth System Sciences, 14, 789-798.

Feng, L., Qu, R., Ji, Y., Zhu, W., Zhu, Y., Feng, Z., Fan, W., Guan, Y. and Xie, C. (2022): Multistationary geomagnetic vertical intensity polarization anomalies for predicting M ≥ 6 Earthquakes in Qinghai, China. Applied Sciences, 12, 17, 8888.

Gonzalez, W.D., Joselyn, J.A., Kamide, Y., Kroehl, H.W., Rostoker, G., Tsurutani, B.T. and Vasyliunas, V.M. (1994): What is a geomagnetic storm?. Journal of Geophysical Research: Space Physics, 99, A4, 5771-5792.

Guzman-Vargas, L., Carrizales-Velazquez, C., Reyes-Ramírez, I., Fonseca-Campos, J., Rosa-Galindo, A.D., Quintana-Moreno, V.O., Peralta, J.A. and Angulo-Brown, F. (2019): A comparative study of geoelectric signals possibly associated with the occurrence of two Ms > 7 EQs in the South Pacific Coast of Mexico. Entropy, 21, 12, 1225.

Han, P., Hattori, K., Hirokawa, M., Zhuang, J., Chen, C.-H., Febriani, F., Yamaguchi, H., Yoshino, C., Liu, J.-Y. and Yoshida, S. (2014): Statistical analysis of ULF seismomagnetic phenomena at Kakioka, Japan, during 2001–2010. Journal of Geophysical Research: Space Physics, 119.

Han, P., Hattori, K., Zhuang, J., Chen, C-H., Liu, J-Y. and Yoshida, S. (2017): Evaluation of ULF seismo-magnetic phenomena in Kakioka, Japan by using Molchan's error diagram. Geophysical Journal International, 208, 482–490.

Han, P., Zhuang, J., Hattori, K., Chen, C. H., Febriani, F., Chen, H., Yoshino, C. and Yoshida, S. (2020): Assessing the potential earthquake precursory information in ULF magnetic data recorded in Kanto, Japan during 2000–2010: Distance and magnitude dependences. Entropy, 22, 8, 859.

Hattori, K., Han, P., Yoshino, C., Febriani, F., Yamaguchi, H. and Chen, C.H. (2013): Investigation of ULF seismo-magnetic phenomena in Kanto, Japan during 2000–2010: case studies and statistical studies. Surveys in Geophysics, 34, 293-316.

Hattori, K., Serita, A., Yoshino, C., Hayakawa, M. and Isezaki, N. (2006): Singular spectral analysis and principal component analysis for signal discrimination of ULF geomagnetic data associated with 2000 Izu Island earthquake swarm. Physics and Chemistry of the Earth, 31, 281–291.

Hayakawa, M and Hattori. (2004): Ultra-low-frequency electromagnetic emissions associated with earthquakes.

IEEJ Transactions on Fundamentals and Materials, 124, 1101–1108.

Hayakawa, M., Hattori, K. and Ohta, K. (2007): Monitoring of ULF (ultra-low-frequency) Geomagnetic Variations Associated with Earthquakes. Sensors, 7, 1108–1122.

Hayakawa, M., Kawate, R., Molchanov, O.A. and Yumoto, K. (1996): Results of ultra-low-frequency magnetic field measurements during the Guam earthquake of 8 August 1993. Geophysical Research Letters, 23, 241-244.

Hayakawa, M., Schekotov, A., Izutsu, J. and Nickolaenko, A.P. (2019): Seismogenic effects in ULF/ELF/VLF electromagnetic waves. International Journal of Electronics and Applied Research, 6, 2, 1-86.

Hayakawa, M., Schekotov, A., Izutsu, J., Yang, S.S., Solovieva, M. and Hobara, Y. (2022): Multi-parameter observations of seismogenic phenomena related to the Tokyo earthquake (M= 5.9) on 7 October 2021. Geosciences, 12, 7, 265.

Heavlin, W.D., Kappler, K., Yang, L., Fan, M., Hickey, J., Lemon, J., MacLean, L., Bleier, T., Riley, P. and Schneider, D. (2022): Case-control study on a decade of ground-based magnetometers in California reveals modest signal 24–72 hr prior to earthquakes. Journal of Geophysical Research: Solid Earth, 127, 10, e2022JB024109.

Hutchings, S.J. and Mooney, W.D. (2021): The seismicity of Indonesia and tectonic implications. Geochemistry, Geophysics, Geosystems, 22, 9, p.e2021GC009812.

Ida, Y., Hayakawa, M. and Gotoh, K. (2006): Multifractal analysis for the ULF geomagnetic data during the Guam earthquake. IEEJ Transactions on Fundamentals and Materials, 126, 4, 215-219.

Mahmoudian, A., Safari, M. and Rezapour, M. (2022): Earthquake prediction assessment using VLF radio signal sounding and space-based ULF emission observation. Acta Geophysica, 70, 1269–1284.

Marzuki, M., Hamidi, M., Ahadi, S., Putra, A., Afdal, A., Harmadi, H., Karnawati, D., Suprihatin, H.S., Syirojudin, M. and Marsyam, I. (2022): ULF geomagnetic anomaly associated with the Sumatra-Pagai Islands earthquake swarm during 2020. Contributions to Geophysics and Geodesy, 52, 22, 185-207.

Morlet, J., Arens, G., Fourgeau, Eliane and Giard, D. (1982): Wave propagation and sampling theory--Part II: Sampling theory and complex waves. Geophysics, 47, 222-236.

Ozsoz, I, and Pamukcu, O.A. (2021): Detection and interpretation of precursory magnetic signals preceding October 30, 2020 Samos earthquake. Turkish Journal of Earth Sciences, 30, 8, 748-757.

Peng, C-K., Buldyrev, S.V., Havlin, S., Simons, M., Stanley, H.E. and Goldberger, A.L. (1994): Mosaic organization of DNA nucleotides. Physical review e, 49, 2, 1685.

Pesicek, J.D., Thurber, C.H., Zhang, H., DeShon, H.R., Engdahl, E.R. and Widiyantoro, S. (2010): Teleseismic double-difference relocation of earthquakes along the Sumatra-Andaman subduction zone using a 3-D model. Journal of Geophysical Research: Solid Earth, 115, B10.

Potirakis, S.M., Contoyiannis, Y., Schekotov, A., Eftaxias, K. and Hayakawa, M. (2021): Evidence of critical dynamics in various electromagnetic precursors. The European Physical Journal Special Topics, 230, 1, 151-177.

Potirakis, S.M., Schekotov, A., Contoyiannis, Y., Balasis, G., Koulouras, G.E., Melis, N.S., Boutsi, A.Z., Hayakawa, M., Eftaxias, K. and Nomicos, C. (2019): On possible electromagnetic precursors to a significant earthquake (Mw= 6.3) occurred in Lesvos (Greece) on 12 June 2017. Entropy, 21, 3, 241.

Ramadhani, A.F., Triyono, R. and Ubaya, T. (2019): Analysis of magnetic field anomalies before earthquakes based on ULF (Ultra Low Frequency) method using magnetic sensor data in Sumatra. Journal of Physics: Conference Series, 1317, 1, 012044.

Saroso, S., Hattori, K., Ishikawa, H., Ida, Y., Shirogane, R., Hayakawa, M., Yumoto, K., Shiokawa, K. and Nishihashi, M. (2009): ULF geomagnetic anomalous changes possibly associated with 2004–2005 Sumatra earthquakes. Physics and Chemistry of the Earth, 34, 343-349.

Singh, V. and Hobara, Y. (2020): Simultaneous study of VLF/ULF anomalies associated with earthquakes in Japan. Open Journal of Earthquake Research, 9, 2, 201-215.

Sokacana, I., Rosid, M.S. and Ahadi, S. (2019): Optimum frequency identification of anomalous geomagnetic signal related to earthquake precursor in Sumatra Island. IOP Conference Series: Earth and Environmental Science, 406, 1, 012021.

Stanica, D.A. and Stanica, D. (2019): ULF pre-seismic geomagnetic anomalous signal related to Mw8.1 offshore Chiapas earthquake, Mexico on 8 September 2017. Entropy, 21, 1, 29.

Stanica, D.A. and Stanica, D. (2021): Possible Correlations between the ULF Geomagnetic Signature and Mw6.4 Coastal Earthquake, Albania, on 26 November 2019. Entropy, 23, 2, 233.

Supendi, P., Widiyantoro, S., Muhari, A., Rawlinson, N., Rohadi, S., Karnawati, D., Hanifa, N.R., Imran, I., Gunawan, E. and Faizal, L. (2022): Potential megathrust earthquakes and tsunamis off the southern coast of West Java, Indonesia. Natural Hazards. 1-14.

Telesca, L., Lapenna, V., Macchiato, M. and Hattori, K. (2008): Investigating non-uniform scaling behavior in Ultra Low Frequency (ULF) earthquake-related geomagnetic signals. Earth and Planetary Science Letters, 268, 1-2, 219-224.

Wang, J.H. (2020): Piezoelectricity as a mechanism on generation of electromagnetic precursors before earthquakes. Geophysical Journal International, 224, 1, 682-700.

Warden, S., MacLean, L., Lemon, J. and Schneider, D. (2020): Statistical analysis of pre-earthquake electromagnetic Anomalies in the ULF Range. Journal of Geophysical Research: Space Physics, 125, 10, e2020JA027955.

Wessel, P., Luis, J. F., Uieda, L., Scharroo, R., Wobbe, F., Smith, W. H. and Tian, D. (2019): The generic mapping tools version 6. Geochemistry, Geophysics, Geosystems, 20, 11, 5556-5564.

Widiyantoro, S. and van der Hilst, R. (1997): Mantle structure beneath Indonesia inferred from high-resolution tomographic imaging. Geophysical Journal International 130, 1, 167-182.

Widiyantoro, S., Gunawan, E., Muhari, A., Rawlinson, N., Mori, J., Hanifa, N.R., Susilo, S., Supendi, P., Shiddiqi, H.A., Nugraha, A.D. and Putra, H.E. (2020): Implications for megathrust earthquakes and tsunamis from seismic gaps south of Java Indonesia. Scientific Reports, 10, 1, 1-11.

Yao, X., Wang, W. and Teng, Y. (2022): Detection of Geomagnetic Signals as Precursors to Some Earthquakes in China. Applied Sciences, 12, 3, 1680.

Yusof, K.A., Abdullah, M., Hamid, N.S., Ahadi, S. and Yoshikawa, A. (2021): Correlations between earthquake properties and characteristics of possible ULF geomagnetic precursor over multiple earthquakes. Universe, 7, 1, 20.

Yusof, K.A., Abdullah, M., Hamid, N.S.A. and Ahadi, S. (2019a): On effective ULF frequency ranges for geomagnetic earthquake precursor. IOP Conference Series: Journal of Physics Conference Series, 1152, 012033.

Yusof, K.A., Hamid, N.S.A., Abdullah, M., Ahadi, S. and Yoshikawa, A. (2019b). Assessment of signal processing methods for geomagnetic precursor of the 2012 M6.9 Visayas, Philippines earthquake. Acta Geophysica, 67, 1297-1306.

### *Papers written in non-English language:*

Sabtaji, A. (2020): Statistik kejadian gempa bumi tektonik tiap provinsi di wilayah Indonesia selama 11 tahun pengamatan (2009-2019) (*Statistics of tectonic earthquake events each province in Indonesia territory for 11 years of observation (2009-2019)*). Buletin Meteorologi, Klimatologi, dan Geofisika, 7, 31-46. (*in Indonesian - English*)

### *Book:*

Molchanov, O.A. and Hayakawa, M. (2008): Seismo-electromagnetics and related phenomena: History and latest results. Terra Scientific Publishing, Tokyo, 189 p.

### *Books written in non-English language:*

Ramdhan, M., Priyobudi, Imananta, R.T., Muzli, Supendi, P., Perdana, Y.H., Nugraha, J., Jatnika, J., Ali, Y.H., Panjaitan, A.L., Nugraha, M.F., Kristyawan, S., Sembiring, A.S., Setyahadi, A.R. and Yogaswara, D.S. (2021): Katalog gempabumi Indonesia: relokasi hiposenter dan implikasi tektonik (*Indonesia earthquake catalog: Hypocenter relocation and tectonic implications*). Pusat Gempabumi dan Tsunami, Badan Meteorologi Klimatologi dan Geofisika (BMKG), Jakarta, 122 p. (*in Indonesian*)

Statistics Indonesia (BPS). (2020): Statistik Indonesia 2020 (*Statistics Indonesia 2020*). Badan Pusat Statistik, Jakarta. (*in Indonesian*)

## SAŽETAK

## Procjena geomagnetskih fenomena ultraniske frekvencije (ULF) povezanih s potresima u zapadnome dijelu otoka Java, Indonezija, tijekom 2020.

Geomagnetska analiza ultraniske frekvencije (ULF) robusna je metoda za predviđanje potresa (EQ). Proveli smo simultanu studiju prekursora potresa oko zapadnoga dijela otoka Java 2020. koristeći se metodom wavelet transformacije (WT) i analize fluktuacije s detrendiranjem (DFA). ULF geomagnetski podatci (od ožujka do prosinca 2020., 16:00 – 21:00 UTC ili 23:00 – 04:00 LT) s geomagnetske postaje Lampung Selatan (LPS) korišteni su za procjenu prekursora. Analizirali smo četiri potresa s udaljenošću epicentra (R) od oko 100 km od postaje Lampung Selatan i magnitudom (M) većom od 5 Mw. Analizirali smo promjene u SZ/SG vrijednostima i α-vrijednostima iz WT i DFA analiza u odnosu na prag (μ±2σ) kako bismo identificirali anomalije povezane s potresima. Rezultat je pokazao da su se anomalije SZ/SG pojavile istodobno sa smanjenjem α-vrijednosti nekoliko tjedana prije vjerojatnoga izvora potresa kada je postojala vrlo niska geomagnetska aktivnost (Dst ≤ -30 nT). Mw 5,4 (7. 7. 2020.) potresa mogao bi biti glavni izvor koji je doveo do pojave prekursora jer je imao najveću magnitudu i KLS vrijednosti u usporedbi s drugima. Kombinirani rezultati WT i DFA pokazali su anomalije 1,5 – 13 tjedana prije Mw 5,4 (7. 7. 2020.) potresa. Rezultati upućuju na to da su WT i DFA prikladne metode za otkrivanje prekursora potresa, ali potrebno je više rada kako bi se prekursori povezali s određenim potresima.

**Ključne riječi:**
prekursori potresa, ULF emisija, analiza *wavelet* transformacije, detrendirana analiza fluktuacije

## Authors' contribution

**Cinantya Nirmala Dewi (1)** (M.Sc) and **Febty Febriani (2)** (Ph.D.) designed the research, conducted wavelet and detrended fluctuation analysis, examined the results, and wrote the manuscript. **Titi Anggono (3)** (Dr.) and **Syuhada (4)** (Dr.) designed one-year $E_S$ and $K_{LS}$ analyses and examined the results. **Mohamad Ramdhan (5)** (Dr.) performed earthquake relocation. **Mohammad Hasib (6)** (Dr.) and **Aditya Dwi Prasetio (7)** (M.Sc) examined the results. **Hendra Suwarta Suprihatin (8)** (B.Sc) **and Suaidi Ahadi (9)** (Dr.) provided geomagnetic data. **Mohammad Nafian (10)** (M.Sc), **Suwondo (11)** (M.Sc)**, and Faiz Muttaqy (12)** (Dr.) designed the research and examined the results. **Muhamad Syirojudin (13)** (Dr.), **Hasanudin (14)** (B.Sc), and **Indah Marsyam (14)** (B.Eng) provided geomagnetic data.